

1 ***Rhizoglopus venetianum*, a new arbuscular mycorrhizal fungal species from a heavy metal contaminated**
2 **site, downtown Venice in Italy**

3 Alessandra Turrini¹, Martina Saran¹, Manuela Giovannetti¹, Fritz Oehl^{2*}

4 ¹Department of Agriculture, Food and Environment, University of Pisa, Via del Borghetto 80, 56124 Pisa, Italy

5 ²Agroscope, Competence Division for Plants and Plant Products, Ecotoxicology, Müller-Thurgau-Strasse 29,
6 CH-8820 Wädenswil, Switzerland.

7

8 ***Corresponding author**

9 Fritz Oehl Agroscope, Competence Division for Plants and Plant Products, Ecotoxicology, Müller-Thurgau-
10 Strasse 29, CH-8820 Wädenswil, Switzerland

11 Email address: fritz.oehl@gmail.com

12

13

14 **Abstract**

15 *Rhizoglopus venetianum*, a new arbuscular mycorrhizal fungal species, has been isolated and propagated from a
16 heavy metal contaminated site in Sacca San Biagio island, downtown Venice, Italy. Interestingly, under the high
17 levels of heavy metals occurring in the site, the new fungus was able to grow only intraradically. In greenhouse
18 trap and single species cultures under low heavy metal levels, the fungus produced innumerable spores, clusters
19 and sporocarps extraradically, which were formed terminally on subtending hyphae either singly, in small spore
20 clusters, or, preferably, in loose to compact non-organized sporocarps up to 2,500 × 2,000 × 2,000 µm. Spores
21 are golden-yellow to bright yellow brown, globose to subglobose to rarely oblong, 75–145 × 72–140 µm in
22 diameter and have four spore wall layers. Morphologically, the new fungus is similar to *R. intraradices*, and
23 phylogenetically it forms a monophyletic clade next to *R. irregulare*, which generally forms irregular spores and
24 lacks, like *R. intraradices*, the flexible innermost wall layer beneath the structural/persistent third wall layer. A
25 key for the species identification is presented comprising all 18 *Rhizoglopus* species, so far described or newly
26 combined.

27

28 **Keywords**

29 Arbuscular mycorrhizal fungi; Heavy metals; *Rhizoglopus*; Morphology; Molecular phylogeny; SSU–ITS–LSU
30 nrDNA

31

32 **Introduction**

33 The number of species of arbuscular mycorrhizal (AM) fungi (AMF, Glomeromycota, Tedersoo et al. 2018)
34 greatly increased during the last decades, passing from about 120 to ca. 300 species since nineties (Schenck and
35 Pérez 1990; Giovannetti et al. 1990; Oehl et al. 2011a; Błaszowski 2012; Krüger et al. 2012). The continuous
36 progress in the morphological identification of AMF species (e.g. Sieverding et al. 2014; Błaszowski et al.
37 2015, 2018) and in the setup of suitable molecular tools based on more informative regions of nuclear rDNA
38 (Silva et al. 2006; Krüger et al. 2009), resolving even very closely related taxa (Stockinger et al. 2010; Krüger et
39 al. 2012), allowed the discovery and separation of new species (ca. 10 per year in the last 20 years), covering
40 diverse genera and families, some ubiquitous, but others rare or associated with particular plants or habitats
41 (Turrini and Giovannetti 2012). However, the huge AMF diversity, evidenced on the basis of environmental
42 DNA sequences, which do not correspond to formally described species (Öpik et al. 2010, 2014), is still far to be
43 fully described. Actually, it was calculated that probably less than 5% of existing AMF in the world have
44 formerly been described so far (Krüger et al. 2009), most of which have not yet been cultivated in pure cultures.
45 Indeed, the difficulty in cultivating AMF out of their original environment still represents one of the major limits
46 to the isolation and description of new species. Nevertheless, AMF research focused on invaluable “hot spots”
47 for species diversity (Myers et al. 2000), distributed around the world, together with studies on AMF occurring
48 in extreme habitats (high-altitude habitat, high-salinity habitat, thermal habitat, desert, wetland, polluted soils)
49 would probably lead to the discovery of novel endemic genetic resources (Turrini and Giovannetti 2012; Sousa
50 et al. 2018). In very recent years, new species were isolated from extreme habitats, i.e. *Rhizoglossum melanum*
51 from wetland (Sudová et al. 2015), *Diversispora omaniana*, *Septoglossum nakheelum* and *Rhizoglossum arabicum*
52 from hyper arid environments of the Arabian Peninsula (Symanczik et al. 2014, 2018), and *Acaulospora*
53 *pustulata* and *Acaulospora tortuosa* from high altitude habitat in Sierra Nevada, Spain (Palenzuela et al. 2013).

54 Among extreme habitats, those contaminated by heavy metals (HM) represent invaluable sites for the
55 recovery of peculiar AMF isolates and species. HM are extremely toxic to microbial communities, modifying the
56 structure of some essential enzymes, causing oxidative damage and DNA injury and altering plasma membranes
57 (Hassan et al. 2011).

58 During last years HM-polluted habitats have been largely studied in relation to AMF occurrence, due to
59 the their beneficial effects in enhancing plant tolerance to such toxic habitats (Pawłowska et al. 1996;
60 Hildebrandt et al. 2007). It has been shown that AMF play a fundamental role in HM phytostabilization and
61 phytoextraction (Gohre and Paszkowski 2006) by trapping HM in their hyphae and spores, and, consequently,
62 reducing metal availability for the plants (González-Chávez et al. 2002, 2009; Cornejo et al. 2013). Many studies

63 have described different AMF communities occurring in HM-polluted soils (Turnau et al. 2001; Vogel-Mikuš et
64 al. 2006; Regvar et al. 2010; Hassan et al. 2011; Ban et al. 2015; Yang et al. 2015, Sánchez-Castro et al. 2017)
65 and in the roots of plants spontaneously growing in HM-polluted areas (Whitfield et al. 2004; Vallino et al.
66 2006; Zarei et al. 2008, Bedini et al. 2010). Molecular analyses of AMF communities of HM-polluted sites
67 detected several sequence types new to science (Vallino et al. 2006; Sánchez-Castro et al. 2017), including
68 sequences from Sacca San Biagio, an ash disposal island located downtown Venice (Italy; Bedini et al. 2010).

69 Sacca San Biagio, which can be considered a model system for the study of remediation and
70 requalification of polluted environments, has been spontaneously colonized by pioneer plants, animals and
71 microorganisms during the past 30 years, since incinerator plant's closure in 1984. Most of the plants occurring
72 on the island showed a high level of AM fungal colonization (67%), but no spores were retrieved in bottom
73 ashes. The molecular analysis, carried out on the roots of three mycorrhizal plants growing on the island,
74 evidenced the occurrence of sequences corresponding to the '*Rhizoglosum intraradices/Rhizoglosum*
75 *fasciculatum*' complex, together with sequences detected so far only *in planta* and sequences new to science
76 (Bedini et al. 2010).

77 The goal of the present work was to obtain in pure culture AMF spores, after transplanting the host
78 plants from Sacca San Biagio island to a non-polluted environment, and to describe a new AM fungal species
79 associated to the ruderal host plant *Senecio inaequidens*. Both morphological and molecular techniques were
80 used to characterize the AM fungus, which was named *Rhizoglosum venetianum*.

81

82 **Material and Methods**

83 **Study site**

84 The new glomeromycotan species originated from Sacca San Biagio island, downtown Venice (latitude 45° 42'
85 N, longitude 12° 30' E). The island is a tideland, that was elevated after the Second World War, filling the
86 lagoon sand with inert construction waste, which has been subsequently covered by bottom ashes produced by
87 an incinerator plant of municipal solid waste (MSW), operating for more than ten years, since 1973 up to 1984.
88 Ashes form layers of about 1.5-3 m and occupy a volume of about 60,000 m³ (Bedini et al. 2010). They are
89 highly toxic, since the incineration process enhances the concentration of some pollutants, especially heavy
90 metals, which represent a risk for human health and the environment (Clijsters et al. 2000). Ashes contains high
91 concentrations of different heavy metals: Al (25,941.6 mg kg⁻¹), As (24.8 mg kg⁻¹), Cd (3.4 mg kg⁻¹), Cr (101.6
92 mg kg⁻¹), Cu (1820.1 mg kg⁻¹), Ni (83.6 mg kg⁻¹), Pb (2000.8 mg kg⁻¹), Zn (3210 mg kg⁻¹) (Bedini et al. 2010).
93 Moreover they contain 85.1% sand, 10.1% silt, 4.8% clay, 5.1% total organic C, a pH (KCl) of 8 and the

94 following total nutrient concentrations: 2.8 ‰ total N, 1215.3 mg kg⁻¹ total P, and 24.6 mg kg⁻¹ available P
95 (Olsen) (Bedini et al. 2010). After the year 1984 the incinerator was demolished and no activities were carried
96 out on the isle, which has been naturally colonized by both herbaceous and woody plants for more than 30 years.
97 Plant communities detected on the isle were mostly ruderal and nitrophilous, (class *Artemisietea vulgaris*,
98 including perennial ruderal xerophilous phytocenoses, typical of temperate or Mediterranean regions) (Mucina et
99 al. 1997). Among plant species occurring in Sacca San Biagio island, *S. inaequidens* plants, belonging to the
100 Asteraceae family, were selected and collected with their intact root system. They are ruderal plants originating
101 from South Africa, very adaptable to different environments, invasive, spreading in many countries also in
102 Europe. *Senecio inaequidens*, widely distributed on the isle at the sampling time, was chosen for spore isolation,
103 since it was shown to be highly mycorrhizal and able to host in its roots different AMF species (Bedini et al.
104 2010).

105

106 **Sampling, establishment and growth of trap and pure cultures.**

107 *Senecio inaequidens* plants and rhizosphere toxic ashes were collected in Sacca San Biagio island in May 2011
108 (Figs 1-2). Plants and ashes were transplanted in 8 L pots filled with a steam-sterilized 1:1 volumetric mixture of
109 agricultural field soil collected at the Interdepartmental Centre for Agri-environmental Research Enrico Avanzi
110 (CIRAA), University of Pisa, S. Piero a Grado, Pisa, Italy (latitude 43° 40' N, longitude 10° 19' E) and
111 TerraGreen (calcinated clay; OILDRI, Chicago, IL, USA), then transferred in greenhouse to induce AMF
112 sporulation of fungi occurring in *S. inaequidens* roots, which were used as "trap cultures" for the isolation of AM
113 fungal spores from the heavy metal toxic island (Fig. 3). At different time points, after 6, 9, 12 months of culture,
114 rhizosphere soil (50 g) from different trap cultures was sieved through a set of nested sieves down to a mesh size
115 of 50 µm (Gerdemann and Nicolson 1963) for spore collection and analysis and the spores were extracted by a
116 water-sucrose gradient and centrifugation (Sieverding 1991). Spores investigated in this study were obtained
117 from spore clusters (max 5 spores connected with a common hypha). Pure cultures were achieved making use of
118 the "sandwich system", useful to allow the interaction between AMF and plant roots (Giovannetti et al. 1993).
119 Briefly, small spore clusters were let to germinate for 10 days in sterile microwells containing sterile water, in a
120 growth chamber at 24°C in the dark. Germinated spores were then placed in contact with the roots of *Trifolium*
121 *alexandrinum* plantlets placed on 47-mm diameter cellulose ester Millipore™ membranes (0.45 µm diameter
122 pores). Another 47-mm membrane was placed on spores and root systems to close the sandwich. The "sandwich
123 system" was buried in sterile 10 cm pots containing steam-sterilized quartz grit, then maintained in
124 suntransparent bags (Sigma, Milan, Italy) under controlled conditions (18-24°C, 16-8-h photoperiod of

125 irradiance $100 \mu\text{Em}^{-2} \text{ s}^{-1}$, 60% RH). Plants were supplied weekly with 10 ml half strength Hoagland's solution.
126 After 6 weeks the "sandwich systems" were opened, plants were gently removed and the occurrence of
127 extraradical mycelium was assessed under a stereomicroscope (Wild, Leica, Milan, Italy) (Figs. 4-5). When
128 colonization check was positive, plants were transferred to 700 cm^3 plastic pots containing a 1:1 mixture of soil
129 and Terragreen, and moved to the greenhouse. Pots were regularly checked for spore formation, as described
130 above. Sporulation was obtained after 4 months of culture (Fig. 6). The new species was maintained and
131 renewed under greenhouse conditions together with *T. alexandrinum* and *Lactuca sativa* as host plants in the
132 International Microbial Archive (IMA) collection of the Department of Agriculture Food and Environment,
133 University of Pisa, Pisa, Italy.

134

135 **Morphological analyses**

136 Spores were isolated from the pot-culture soil by wet sieving and decanting through a set of nested sieves down
137 to a mesh size of $32 \mu\text{m}$ (Sieverding 1991), then transferred into Petri dishes and examined under a
138 stereomicroscope (Wild, Leica, Milan, Italy). Spores were isolated by using capillary pipettes, mounted on
139 microscope slides in polyvinyl alcohol lacto-glycerol (PVLG; Koske and Tessier 1983), in PVLG + Melzer's
140 reagent (1:1, v:v; Brundrett et al. 1994) and in water (Spain 1990). Qualitative spore traits (sporocarp and spore
141 shape, color and size, spore wall structure, including color and size of each wall layer of the spores and their
142 subtending hyphae) were examined on > 25 sporocarps and > 100 spores.

143 The terminology of the spore structure basically is that presented for species with glomoid spore
144 formation in Oehl et al. (2011b), Sieverding et al. (2014) and Błaszowski et al. (2018). Photographs were taken
145 with a digital camera (Leica DFC 295) on a stereomicroscope (Leica S8APO) and a compound microscope
146 (Leica DM750) using Leica Application Suite Version V4.1 software. Specimens mounted in PVLG and a (1:1)
147 mixture of PVLG and Melzer's reagent were deposited at Z+ZT (ETH Zurich, Switzerland), and at the Botanical
148 Garden of the University of Pisa, Italy.

149

150 **Molecular analysis and phylogeny**

151 Intact, healthy spores were manually collected with a capillary pipette under a dissecting microscope (Wild,
152 Leica) and cleaned by sonication (120 s) in a B-1210 cleaner. After three rinses in sterile distilled water (SDW),
153 spores were surface sterilised with 2% chloramine T supplemented with streptomycin ($400 \mu\text{g/ml}$) for 20 min
154 and rinsed five times in SDW. Intact sterilized single spores were selected under a laminar flow hood,
155 individually transferred into Eppendorf PCR tubes, crushed with a glass pestle and their DNA directly amplified

156 using the nested protocol of Krüger et al. (2009), focused on a fragment of about 1500 bp covering partial SSU,
157 the whole ITS and the D1 and D2 variable regions of the LSU sequences of rDNA. In the first PCR reaction
158 crushed spores were amplified in 25 µl of PCR reaction mix using 0.125 U GoTaq Flexi DNA Polymerase
159 (Promega, Milan, Italy), 0.4µM of each primer (SSUmAf1 and LSUmAr3, Krüger et al. 2009), 0.2 mM (each)
160 dNTPs, 1.5 mM MgCl₂ and 1× manufacturer's reaction buffer. The thermal cycler was programmed as follows:
161 a manual hot start at 95°C for 3 min, 35 cycles at 95°C for 30 s, 60°C for 1 min, 72°C for 2 min and a final
162 extension step at 72°C for 10 min. The nested PCR reactions were performed by diluting (1:100) the first PCR
163 amplicons and using 2 µl of dilutions as template for the second reaction in a final volume of 50 µl. The primer
164 pair, SSUmCf1-LSUmBr3 (Krüger et al. 2009; 0.4µM), was added to the PCR mix. Taq DNA polymerase,
165 dNTPs, buffer and MgCl₂ concentrations were the same as those described above. Amplification conditions
166 were as follows: a manual hot start at 95°C for 3 min, 35 cycles at 95°C for 30 s, 63°C for 45 s, 72°C for 1,5 min
167 and a final extension step at 72°C for 10 min. PCR products (10 µl) were separated on 1% agarose gels
168 containing ethidium bromide (0.5 µg/ml).

169 Amplified DNA fragments of SSU-ITS-LSU regions were purified by Wizard SV Gel and PCR Clean-
170 Up System according to the manufacturer's instructions (Promega), with a final elution volume of 20 µl and
171 purified products (2 µl) were quantified by a BioPhotometer (Eppendorf). Purified products were cloned into
172 pGem®-T Easy vector according to the manufacturer's instructions (Promega). Putative positive clones were
173 screened by standard SP6/T7 amplifications, followed by a nested PCR using the SSUmCf1-LSUmBr3 primer
174 pair. Concentration of PCR mix components and PCR conditions were the same as those described above for
175 PCR reactions. Six clones from single spores (two clones/spore) were purified by Wizard® Plus SV Minipreps
176 (Promega). Recombinant plasmids were sequenced using SP6/T7 vector primers at GATC Biotech (Köln,
177 Germany). Sequences reported in this study were deposited in the European Nucleotide Archive
178 (<http://www.ebi.ac.uk/ena>) under the accession numbers LS974594-LS974599. The alignment for the tree
179 obtained in this study was deposited at TreeBase under the ID: 23045.

180 Sequences were edited in MEGA6 (Tamura et al. 2013) and their similarities determined using the
181 Basic Local Alignment Search Tool (BLASTn) provided by NCBI. Then they were aligned with those
182 corresponding to the closest matches from GenBank as well as with some sequences from the Glomeraceae
183 family covering the entire SSU-ITS-LSU region or portion thereof, using MUSCLE as implemented in MEGA6.
184 Phylogenetic tree was inferred by Bayesian and Maximum-likelihood analyses. The Bayesian analysis was
185 carried out in MrBayes version 3.2 (Ronquist et al. 2012), using the General Time Reversible sequence
186 evolutionary model and branch support values corresponded to the posterior probabilities of two Markov chain

187 Monte Carlo samplings over 500,000 generations and a tree sampling every 100 generations after discarding the
188 initial 10%. For the maximum-likelihood analysis the evolutionary rate differences among sites were computed
189 in MEGA6 using a discrete Gamma distribution + G method. The confidence of branching was assessed using
190 1000 bootstrap resamplings. The generated phylogenetic tree was drawn in MEGA6 and edited in Adobe
191 Acrobat XI.

192

193 **Results**

194 **Taxonomic analyses**

195 ***Rhizoglosum venetianum*** Oehl, Turrini, & Giovann., **sp. nov.**, Figs 7–18

196 MYCOBANK MB 825301

197 DIAGNOSIS - Differs from *Rhizoglosum irregulare* and *R. intraradices* by having an additional, fourth
198 wall layer, below the structural wall layer.

199 ETYMOLOGY: *venetianum* referring to the city of Venice to which the island Sacca San Biagio belongs.

200 TYPE: Holotype, deposited at Z+ZT (accession ZT Myc 58970), derived from a pure culture established
201 on the host plant *Trifolium alexandrinum* in the greenhouse of the Microbiology Laboratory in Pisa, at the
202 Department of Agriculture, Food and Environment, University of Pisa, Italy. Mycorrhizal mycelia and
203 intraradical mycorrhizal structures, occurring in the roots of *Senecio inaequidens* plants, were collected in Sacca
204 San Biagio island in the central lagoon of Venice Italy (45°25'36''N; 12°18'34''E). The island hosted a
205 Municipal Solid Wastes incinerator operating since 1973 up to 1984, producing bottom ashes that were disposed
206 all over the island area. Since 1984 no significant activities were carried out on the island and in 2003 the
207 furnace was demolished. In the last 30 years the highly polluted soil of the island has been naturally colonized by
208 spontaneous vegetation. Collector of the host plant *S. inaequidens* was A. Turrini and collection date 31.05.2011.
209 Isotypes deposited at Z+ZT (ZT Myc 58971) and at the Botanical Garden of the University of Pisa (PI-MH-Z11
210 to Z18). The living culture is currently maintained in the International Microbial Archives in Pisa under the
211 accession number IMA10.

212 DESCRIPTION: Spores formed terminally on subtending hyphae (SH) either singly, in small spore
213 clusters, or, preferably, in loose to compact non-organized sporocarps with (10–)40–150 up to hundreds to a few
214 thousands of spores per sporocarp, with sporocarps up to 2,500 × 2,000 μm. Large sporocarps may consist of
215 several small sporocarps. Spores are golden yellow-brown to yellow brown, globose to subglobose to rarely
216 oblong or rarely irregular, (75–)85–130(–145) × (72–)84–125(–140) μm. Mycelial hyphae staining pinkish to
217 purple in Melzer's reagent.

218

219 Spore wall has four layers. Outer layer (SWL1) is hyaline, evanescent, 0.6–1.3 μm thick. Second layer
220 (SWL2) is hyaline to subhyaline, evanescent, 0.8–1.4 μm thick. Third layer (SWL3) is structural, persistent,
221 laminate, golden-yellow to bright yellow brown, 2.0–3.5 μm thick, expanding up to 7.5 μm under pressure in
222 lactic acid based mountants. Innermost layer (SWL4) flexible, light-yellow to bright yellow, 0.6–1.4 μm thick,
223 usually tightly adherent to SWL3, sometimes separating or showing several folds in crushed spores. In Melzer's
224 reagent, SWL1 and SWL2 stain pinkish to pinkish purple, while SWL3 stain purple.

225 Subtending hyphae (SH) of spores cylindrical to slightly funnel-shaped, sometimes recurved, 9.1–13.2
226 μm broad and 15–100 μm long, and without introverted wall thickening toward the spore base. The base
227 generally is not closed by a septum formed by SWL3 or SWL4 but open. Such septa can more often be found in
228 some distance from the spore bases within the intrasporocarpic hyphae (ISH), which are 8–15 μm thick, golden
229 yellow to bright yellow brown. SWL2-4 continue in the ISH. The extrasporocarpic hyphae (ESH, or mycelia
230 hyphae) are hyaline, 5–12 μm thick and have 1–2 hyphal wall layers. In the transition zone between ISH and
231 ESH hyphae are slightly pigmented and generally show several septa within a rather short distance of 100 to 200
232 μm .

233 MYCORRHIZA FORMATION: forming AM associations with *Trifolium alexandrinum* L. and *Lactuca*
234 *sativa* as plant host in pot cultures. The mycorrhizal structures consist of arbuscules, vesicles, and intra- and
235 extraradical hyphae and stain dark blue in 0.05% trypan blue.

236

237 **Molecular analyses**

238 Phylogenetic analyses of the partial SSU, ITS and the partial LSU of the rDNA placed *R. venetianum* sequences
239 in the genus *Rhizoglosum* Sieverd. et al., typified by *R. intraradices* (N.C. Schenck & G.S. Sm.) Sieverd. et al.
240 (Sieverding et al. 2014). Sequences of the new species formed a separate, strongly supported clade (BI = 0.99;
241 ML =95%), sister to that comprising *Rhizoglosum irregulare* (Fig. 19). Actually, blast analyses showed 95-98%
242 homology with *R. irregulare* sequences (isolates DAOM197198, MUCL46241, accession numbers HE817882,
243 FR750130), representing the closest species in our molecular analyses.

244

245 **Erection of a new combination in *Rhizoglosum***

246 In this paragraph, a recently described species, *Rhizophagus neocaledonicus* (Crossay et al. 2018), which
247 morphological and phylogenetically belongs to the genus *Rhizoglosum*, is transferred to *Rhizoglosum* in a new
248 combination:

249 ***Rhizoglomus neocaledonicum*** (D. Redecker, Crossay & Cilia) Oehl, Turrini & Giovann. **comb. nov.**

250 MycoBank 827095

251 Basionym: *Rhizophagus neocaledonicus* D. Redecker, Crossay & Cilia, Mycological Progress 17: 739.

252 2018. <https://doi.org/10.1007/s11557-018-1386-5>.

253

254 **Key to the species in *Rhizoglomus***

255 Here, we are presenting an updated morphological identification key for all 18 species belonging to the genus

256 *Rhizoglomus* according to Sieverding et al. (2014), including the recently described or newly combined species

257 *Rh. dunense*, *Rh. vesiculiferum* and *Rh. neocaledonicum* (e.g. Sieverding et al. 2014; Al-Yahya'ei et al. 2017;

258 Błaszowski et al. 2018):

259 1 Species with two spore wall layers: 2

260 1 Species with > two spore wall layers: 3

261 2 Spores whitish yellow to yellow; species with 1–2 laminae on structural wall layer: 4

262 2 Spores light brown to red brown; 50–90 µm in diam, globose to subglobose, formed singly, in small clusters or

263 large, dense sporocarps (up to 15 × 10 × 10 mm); SWL1 hyaline, evanescent, 1–1.5 µm; SWL2 red to dark

264 brown, 3–6 µm, with several laminae: *R. invermaium* (I.R. Hall) Sieverd., G.A. Silva & Oehl

265 3 Species with three spore wall layers: 5

266 3 Species with > three spore wall layers: 6

267 4 Spores generally < 50 µm; whitish yellow to yellow, 15–50 µm in diam, globose to subglobose, formed singly

268 or in clusters; SWL1 hyaline to light yellow, evanescent, 0.5–1.2 µm; SWL2 whitish yellow to yellow, 0.5–2.0

269 µm: *R. microaggregatum* (Koske, Gemma & P.D. Olexia) Sieverd., G.A. Silva & Oehl

270 4 Spores generally > 50 µm; hyaline to yellow, 60–110 µm in diam, globose to subglobose, formed in small

271 clusters to dense sporocarps, up to 1.8 x 1.4 x 1.4 mm; SWL1 hyaline, evanescent, 0.5–1.2 µm.; SWL2 yellow to

272 yellow brown, 1.2–2.4 µm, consisting of two laminae, that might separate under pressure applied: *R. aggregatum*

273 (N.C. Schenck & G.S. Sm.) Sieverd., G.A. Silva & Oehl

274 5 SWL3 is structural, laminate layer: 7

275 5 SWL3 is flexible layer, adherent to structural, laminate layer SWL2: 8

276 6 Spores generally < 75 µm; spores hyaline to yellowish white or subhyaline, 40–75 µm, globose to subglobose,

277 formed in clusters; spore wall with four layers, 3.3–5.8 µm in total, SWL1 & SWL2 2.5–3.0 µm in total, SWL3

278 & SWL4 laminate, but each is only 0.5–1.0 µm thick: *R. proliferum* (Dalpé & Declerck) Sieverd., G.A. Silva &

279 Oehl

280 6 Spores generally > 75 µm: 9

281 7 Spores yellowish white to yellow brown: 10

282 7 Spores chestnut brown to dark brown; 137–285 µm in diameter, globose to subglobose, formed singly or in
283 small clusters; SWL1 is evanescent, hyaline, 0.8–1.2 µm thick; SWL2 is semi-persistent to evanescent, 2.8–5.1
284 µm thick and shows many fissures in degraded stages. Under pressure on the cover slide single, irregular pieces
285 of SWL2 (about 5–15 × 5–15 µm) may split from the spore surface. SWL3 is dark chestnut brown to black
286 brown, laminate, 7.2–12 µm thick: *R. melanum* Sudová, Sýkorová & Oehl

287 8 Spores generally < 90 µm: 11

288 8 Spores generally > 90 µm: 12

289 9 Spores without flexible inner layer beneath the pigmented, structural layer: 13

290 9 Spores with flexible inner layer beneath the pigmented, structural layer: 14

291 10 Spores ovoid, oblong to often irregular; hyaline to pale yellow, 60–130 × 80–240 µm; they may have deep
292 wall depressions and apical cap-like swellings; SWL1 (0.5–1.5 µm thick) & SWL2 (0.6–5.0 µm thick) hyaline
293 and semi-permanent; SWL3 hyaline to pale yellow, with inseparable laminae, 1.5–4.4 µm thick, staining pale
294 orange to deep red in Melzer's reagent: *R. irregulare* (Błaszcz., Wubet, Renker & Buscot) Sieverd., G.A. Silva &
295 Oehl

296 10 Spores usually globose to subglobose, rarely irregular, without deep wall depressions and apical cap-like
297 swellings: 15

298 11 Spores hyaline to creamy, 70–90 µm, globose to subglobose, formed singly, in clusters or large sporocarps,
299 SWL1 hyaline, 0.5–1.2 µm, evanescent; SWL2 laminate, 2.0–7.5 µm, persistent; SWL3 (semi-)flexible, 0.5–1.4
300 µm thick; all layers staining dark purple in Melzer's: *R. fasciculatum* (Thaxt.) Sieverd., G.A. Silva & Oehl

301 11 Spores dark chestnut to coffee brown, mostly globose to subglobose, 61–83 µm in diam; SWL1 hyaline,
302 mucilaginous, SWL2 laminate, dark brown, 5.4–6.5 µm thick, SWL3 fine, tightly attached to SWL2, sub-hyaline
303 to bright brown: *Rh. neocaledonicum* (D. Redecker, Crossay & Cila) Oehl, Turrini & Giovann.

304 12 Spores generally > 100 µm, hyaline or white to creamy or light yellow to brownish yellow: 16

305 12 Spores 50–70 µm, yellow to yellow brown, globose to subglobose, formed singly, in clusters or sporocarps,
306 1.0 × 0.6 × 0.5 mm; three layered wall up to 12 µm thick; SWL1 hyaline, 0.8–2.0 µm, evanescent; SWL2 light
307 brown, laminate, 4.0–8.0 µm; SWL3 hyaline, 1.5–2.0 µm thick: *R. antarcticum* (Cabello) Sieverd., G.A. Silva &
308 Oehl

309 13 Hyaline outer spore wall layers difficult to differentiate; spores pale yellow to brownish yellow, 110–172 µm,
310 globose to subglobose, formed singly or in small clusters (2–5 spores); SWL1 hyaline, mucilaginous, 0.8–2.5 µm

311 thick, reddish in Melzer's, SWL2 hyaline, rigid, 1.6–2.8 μm thick, SWL3 hyaline to pale yellow, semi-flexible,
 312 easily separated from SWL2, 1.5–2.0 μm thick, non reactive to Melzer's reagent; SWL4 yellow to brownish
 313 yellow, laminated, 2.6–3.8 μm thick, staining dark red in Melzer's: *R. custos* (C. Cano & Dalpé) Sieverd., G.A.
 314 Silva & Oehl
 315 13 Pigmented inner wall layer separating into several layers/laminae under pressure; spores, pale yellow to
 316 grayish yellow, 30–85 \times 50–125 μm , globose to subglobose, formed in clusters up to 0.8 \times 1.0 mm; SW difficult
 317 to interpret; SWL1 hyaline, evanescent, 0.6–2.5 μm , SWL2 readily separating in 2–4 laminae, which might be
 318 counted as SWL2-5, in total up to 5.5 μm thick: *R. arabicum* (Błaszcz., Symanczik & Al-Yahya'ei) Sieverd.,
 319 G.A. Silva & Oehl
 320 14 Spores pastel yellow to light yellow, 75–131 μm , globose to subglobose, formed single or in loose clusters up
 321 to 1.2 mm in diam; SWL1 hyaline, semi-permanent, 1.0–5.3 μm ; SWL2 hyaline, permanent and unit, 0.8–1.5
 322 μm ; SWL3 laminate, pastel yellow to light yellow, 6.3–14.0 μm , consisting of laminae up to 0.8–1.0 μm thick,
 323 frequently easily separating from each other in crushed spores; SWL4 hyaline and flexible, 0.8–2.0 μm . SWL1
 324 and SWL3 stain reddish white to greyish red and brownish violet to violet brown in Melzer's reagent,
 325 respectively: *R. natalense* (Błaszcz., Chwat & B.T. Goto) Sieverd., G.A. Silva & Oehl
 326 14 Spores golden-yellow to bright yellow brown, globose to subglobose, 75–145 \times 72–140 μm in diam, formed
 327 singly, in small spore clusters, or, preferably, in loose to compact sporocarps up to 2.5 \times 2.0 \times 2.0 mm; SWL1,
 328 hyaline, evanescent, 0.6–1.3 μm thick; SWL2, hyaline, evanescent, 0.8–1.4 μm thick; SWL3 structural,
 329 persistent, laminate, golden-yellow to bright yellow brown, 2.0–3.5 μm thick, expanding up to 7.5 μm under
 330 pressure in lactic acid based mountants; SWL4 flexible, light-yellow to bright yellow, 0.6–1.4 μm thick, usually
 331 tightly adherent to SWL3, sometimes separating or showing several folds in crushed spores. In Melzer's reagent,
 332 SWL1 and SWL2 stain pinkish, while SWL3 stain purple: *R. venetianum* Oehl, Turrini, & Giovann.
 333 15 Spores colourless, hyaline, 39–125 μm , globose to subglobose, formed singly in soils; SWL1 semi-
 334 permanent, smooth or slightly roughened, 1.0–5.0 μm ; SWL2 finely laminate, 4.0–8.8 μm ; SWL3 uniform, to
 335 laminate, when up to 2.0 μm thick, (semi-)flexible; SWL1 stains pinkish white to dark red in Melzer's, while
 336 SWL3 turns pale yellow: *R. dunense* Błaszcz. & Kozłowska
 337 15 Spores pigmented, pastel yellow to light yellow or yellow brown to grey brown: 17
 338 16 Spores hyaline (to white), becoming, whitish yellow with age, 120–290 μm , globose to subglobose, formed
 339 singly or in loose clusters; SWL1 1.2–2.3 μm , evanescent to semi-persistent, staining purple in Melzer's, SWL2
 340 5–20 μm laminate, persistent; SWL3 2.0–9.0 μm , often becoming yellow with age: *R. clarum* (T.H. Nicolson &
 341 N.C. Schenck) Sieverd., G.A. Silva & Oehl

342 16 Spores light yellow to brownish yellow, 145–450 μm , globose to subglobose, formed singly or in loose
343 clusters; SWL1 hyaline, evanescent, 2.0–5.0 μm , staining light purple in Melzer's; SWL2 hyaline to light yellow,
344 persistent, 10–16 μm ; SWL3 yellow to yellow brown, flexible, consisting of 1–2 laminae, 0.5–2.0 μm : *R.*
345 *manihotis* (R.H. Howeler, Sieverd. & N.C. Schenck) Sieverd., G.A. Silva & Oehl
346 17 Spores pastel yellow to light yellow, globose, (69–)90(–108) μm diam., rarely egg-shaped, 75–83 \times 80–91
347 μm , formed in loose clusters of 4–18 spores (Błaszowski et al. 2018) or in sporocarps up to 13 \times 10 mm in
348 diam (Thaxter 1922; Gerdemann and Trappe 1974), rarely singly in soil; SWL1 finely-laminate, semi-
349 permanent, hyaline, (1.8–)3.1(–4.5) μm thick, usually slightly swelling in PVLG. SWL2 uniform (not divided
350 into visible sublayers), permanent, hyaline, (1.0–)1.3(–2.3) μm thick, tightly adherent to layer 3, usually difficult
351 to see; SWL3 laminate, permanent, pastel yellow to light yellow, (10.5–)12.0(–13.0) μm thick; the laminae
352 usually easily separate from each other even in spores slightly crushed in PVLG; SWL1 staining yellowish white
353 to pale yellow, SWL2 yellowish red to reddish white & SWL3 staining dark ruby in Melzer's reagent: *Rh.*
354 *veisculiferum* (Thaxt.) Błasz., Kozłowska, Niezgoda, B.T.Goto & Dalpé
355 17 Spores yellow brown to grey brown, often with a greenish tint, 90–135 μm , globose to subglobose, without
356 depressions or swelling at the spore apex, formed singly, in clusters or sporocarps; SWL1 (0.5–1.3 μm thick) &
357 SWL2 (0.8–2.0 μm thick) hyaline and evanescent; SWL3 yellow brown to grey brown, laminate, 3.2–12 μm
358 comprises frequently separating sublayers, which are each 0.5–1 μm thick; SWL1 staining purple in Melzer's
359 reagent: *R. intraradices* (N.C. Schenck & G.S. Sm.) Sieverd., G.A. Silva & Oehl

360

361 Discussion

362 The new AM fungus *Rhizoglopus venetianum* can be easily distinguished from all other *Rhizoglopus* spp. by
363 the combination of spore size, color and spore wall structure. It forms a four-layered spore wall, such as *R.*
364 *natalense*, *R. custos* and *R. proliferum*, which form either smaller spores (*R. proliferum*; < 75 μm), spores of a
365 different spore wall structure (*R. custos*) or less-pigmented spores (*R. natalense*; light yellow to bright yellow
366 spores; see identification key above). Morphologically it resembles *R. intraradices*, which lacks, as also known
367 for *R. irregulare*, the innermost, fourth spore wall layer, which is always present in *R. venetianum*.

368 *R. venetianum* is a fungus isolated from a very toxic environment, containing high levels of heavy
369 metals, especially Zn, Pb and Cu, the latter occurring at very high concentrations, compared with other metal
370 polluted environments in which studies on AMF diversity were performed (Turnau et al., 2001; Vallino et al.,
371 2006; Abdel-Azeem et al., 2007; Khade et al. 2009; Long et al. 2010; Alguacil et al. 2011; Hassan et al. 2011;
372 Krishnamoorthy et al. 2015). Interestingly, also another new species in the genus *Rhizoglopus* (*R. custos*) was

373 isolated from a naturally heavy-metal polluted environment, i.e. the bank side of the Rio Tinto River in southern
374 Spain (Cano et al. 2009), showing high levels of Fe (2g/L), Mg (1.3g/L), Cu (390 mg/L), Zn (280 mg/L) and Mn
375 (100 mg/L). *R. custos*, as *R. venetianum*, forms a multi-stratified wall structure, a trait that might represent a
376 possible barrier to toxic elements for the spores and might help the survival of the species in very toxic
377 environments. Other species in the genus *Rhizoglossus*, such as *R. clarum* or *R. intraradices*, have been shown to
378 possess different attributes linked to the ability of developing strategies, such as avoidance,
379 compartmentalization or resistance to stress, allowing them to live and grow in environments with high levels of
380 heavy metals (Ferrol et al. 2009). Such traits, accompanied with the attitude of Glomeraceae to colonize roots by
381 hyphal fragments or pieces of mycorrhizal roots rather than by germinated spores, might have helped also *R.*
382 *venetianum* to be more competitive and widespread in the roots of *S. inaequidens* plants collected on the island.
383 Interestingly, on Sacca San Biagio, *R. venetianum* appeared to grow entirely intraradically, since no spores of
384 any AMF species were previously detected within ashes (Bedini et al. 2010). We can speculate that AM fungal
385 species, living in very disturbed soil, may complete their life cycle in a privileged ecological niche (within plant
386 roots), avoiding the direct contact with toxic compounds. In our previous study on AMF diversity occurring on
387 Sacca San Biagio (Bedini et al. 2010), the most abundant sequence types detected in the roots of three plant
388 species collected on the island corresponded to *R. irregulare*/*R. fasciculatum* and to *R. intraradices*. Since SSU
389 sequences encompassing the V3-V4 region were not analyzed in this work, we are not able to confirm the
390 occurrence of *R. venetianum* within the VeGlo8 cluster of our previous work. The genus *Rhizoglossus*, to which
391 the identification key to species is proposed in this work, is the prevalent genus in studies on AMF diversity
392 occurring in HM-contaminated sites, since it was dominant in colonized roots of *Fragaria vesca* L. collected in
393 zinc wastes in southern Poland (Turnau et al. 2001), in a HM-contaminated soil along South Tyne River
394 (Whitfield et al. 2004), in a chemical industry contaminated site in Northern Italy (Vallino et al. 2006), in soils of
395 mines in Asia (Zarei et al. 2008; Yang et al. 2015; Sun et al. 2016; Wu et al. 2010; Wei et al. 2015; Park et al.
396 2016) and Europe (Alguacil et al. 2011; del Mar Montiel-Rozas et al. 2017; Sanchez-Castro et al. 2017).

397 In conclusion, Sacca San Biagio represents an interesting site, contributing to our knowledge of AMF
398 diversity in extreme habitats. Future works will disclose the concentrations of heavy metals able to inhibit the
399 growth of the isolate *R. venetianum* IMA10, compared with other AMF species and isolates, and the occurrence
400 of the new fungus in other environments.

401

402 **Acknowledgements**

403 The authors thank Stefano Bedini for his technical assistance and for his help in the field. The authors gratefully
404 acknowledge the financial support by the University of Pisa (Fondi di Ateneo) and SNF (Bern, project
405 IZ7370_152740).

406

407 **References**

408 Abdel-Azeem AM, Abdel-Moneim TS, Ibrahim ME, Hassan MAA, Saleh MY (2007) Effects of long-term
409 heavy metal contamination on diversity of terricolous fungi and nematodes in Egypt-a case study. *Wat Air*
410 *Soil Pollut* 186:233–254. <https://doi.org/10.1007/s11270-007-9480-3>

411 Al-Yahya'ei MN, Mullath SK, AlDhaheiri LA, Kozłowska A, Błaszowski J (2017) *Dominikia emiratia* and
412 *Rhizoglosum dunense*, two new species in the Glomeromycota. *Botany* 95:629–639.
413 <https://doi.org/10.1139/cjb-2016-0294>

414 Alguacil MM, Torrecillas E, Caravaca F, Fernández DA, Azcón R, Roldán A (2011) The application of an
415 organic amendment modifies the arbuscular mycorrhizal fungal communities colonizing native seedlings
416 grown in a heavy-metal-polluted soil. *Soil Biol Biochem* 43:1498–1508.
417 <https://doi.org/10.1016/j.soilbio.2011.03.026>

418 Ban Y, Xu Z, Zhang H, Chen H, Tang M (2015) Soil chemistry properties, translocation of heavy metals, and
419 mycorrhizal fungi associated with six plant species growing on lead–zinc mine. *Ann Microbiol* 65:503–515.
420 <https://doi.org/10.1007/s13213-014-0886-z>

421 Bedini S, Turrini A, Rigo C, Argese E, Giovannetti M (2010) Molecular characterization and glomalin
422 production of arbuscular mycorrhizal fungi colonizing a heavy metal polluted ash disposal island, downtown
423 Venice. *Soil Biol Biochem* 42:758–765. <https://doi.org/10.1016/j.soilbio.2010.01.010>

424 Błaszowski J (2012) Glomeromycota. W. Szafer Institute of Botany, Polish Academy of Sciences, Kraków,
425 Poland.

426 Błaszowski J, Chwat G, Góralska A, Ryska P, Kovács GM (2015) Two new genera, *Dominikia* and *Kamienska*,
427 and *D. disticha* sp. nov. in Glomeromycota. *Nova Hedwigia* 100:225–238.
428 https://doi.org/10.1127/nova_hedwigia/2014/0216

429 Błaszowski J, Kozłowska A, Niezgodą P, Goto BT, Dalpé Y (2018) A new genus, *Oehlia* with *Oehlia*
430 *diaphana* comb. nov. and an emended description of *Rhizoglosum vesiculiferum* comb. nov. in the
431 Glomeromycotina. *Nova Hedwigia*, available online. https://doi.org/10.1127/nova_hedwigia/2018/0488

432 Brundrett M, Melville L, Peterson L (1994) Practical methods in mycorrhizal research. Mycologue Publications,
433 University of Guelph, Guelph

434 Cano C, Bago A, Dalpé Y (2009) *Glomus custos* sp. nov., isolated from a naturally heavy metal-polluted
435 environment in southern Spain. *Mycotaxon* 109:499–512. <https://doi.org/10.5248/109.499>

436 Clijsters H, Vangronsveld J, van der Lelie N, Colpaert J (2000) Ecological aspects of phytostabilization of heavy
437 metal contaminated soils. In: Ceulemans R, Bogaert J, Deckmyn G, Nijs I (eds) *Structure and function in*
438 *plants and ecosystems*. University of Antwerp, UIA, Wilrijk, Belgium, pp 299–306.

439 Cornejo P, Pérez-Tienda J, Meier S, Valderas A, Borie F, Azcón-Aguilar C, Ferrol N (2013) Copper
440 compartmentalization in spores as a survival strategy of arbuscular mycorrhizal fungi in Cu-polluted
441 environments. *Soil Biol Biochem* 57:925–928. <https://doi.org/10.1016/j.soilbio.2012.10.031>

442 Crossay T, Cilia A, Cavaloc Y, Amir H, Redecker D (2018) Four new species of arbuscular mycorrhizal fungi
443 (Glomeromycota) associated with endemic plants from ultramafic soils of New Caledonia. *Mycol Progress*
444 17:729–744. <https://doi.org/10.1007/s11557-018-1386-5>

445 del Mar Montiel-Rozas M, López-García Á, Madejón P, Madejón E (2017) Native soil organic matter as a
446 decisive factor to determine the arbuscular mycorrhizal fungal community structure in contaminated soils.
447 *Biol Fertil Soils* 53:327–338. <https://doi.org/10.1007/s00374-017-1181-5>

448 Ferrol N, González-Guerrero M, Valderas A, Benabdellah K, Azcón-Aguilar C (2009) Survival strategies of
449 arbuscular mycorrhizal fungi in Cu-polluted environments. *Phytochem Rev* 8:551–559.
450 <https://doi.org/10.1007/s11101-009-9133-9>

451 Gerdemann JW, Nicolson TH (1963) Spores of mycorrhizal *Endogone* species extracted from soil by wet sieving
452 and decanting. *Trans Br Mycol Soc* 46:235–246

453 Gerdemann JW, Trappe JM (1974) The *Endogonaceae* in the Pacific Northwest. *Mycol Mem* 5:1–76.

454 Giovannetti M, Avio L, Salutini L (1990) Morphological, cytochemical, and ontogenetic characteristics of a new
455 species of vesicular-arbuscular mycorrhizal fungus. *Can J Bot* 69:161–169.

456 Giovannetti M, Sbrana C, Avio L, Citernesi AS, Logi C (1993) Differential hyphal morphogenesis in arbuscular
457 mycorrhizal fungi during pre-infection stages. *New Phytol* 125:587–594. <https://doi.org/10.1111/j.1469-8137.1993.tb03907.x>

459 Göhre V, Paszkowski U (2006). Contribution of the arbuscular mycorrhizal symbiosis to heavy metal
460 phytoremediation. *Planta* 223:1115–1122. <https://doi.org/10.1007/s00425-006-0225-0>

461 González-Chávez C, D’Haen J, Vangronsveld J, Dodd JC (2002) Copper sorption and accumulation by the
462 extraradical mycelium of different *Glomus* spp. (arbuscular mycorrhizal fungi) isolated from the same
463 polluted soil. *Plant Soil* 240:287–297. <https://doi.org/10.1023/A:1015794622592>

464 González-Chávez MC, Carrillo-Gonzalez R, Gutierrez-Castorena MC (2009) Natural attenuation in a slag heap
465 contaminated with cadmium: the role of plants and arbuscular mycorrhizal fungi. *J Hazard Mat* 161:1288–
466 1298. <https://doi.org/10.1016/j.jhazmat.2008.04.110>

467 Hassan SED, Boon E, St-Arnaud M, Hijiri M (2011) Molecular biodiversity of arbuscular mycorrhizal fungi in
468 trace metal-polluted soils. *Mol Ecol* 20:3469–3483. <https://doi.org/10.1111/j.1365-294X.2011.05142.x>

469 Hildebrandt U, Regvar M, Bothe H (2007) Arbuscular mycorrhiza and heavy metal tolerance. *Phytochemistry*
470 68:139–146. <https://doi.org/10.1016/j.phytochem.2006.09.023>

471 Khade SW, Adholeya A (2009) Arbuscular mycorrhizal association in plants growing on metal-contaminated
472 and noncontaminated soils adjoining Kanpur tanneries, Uttar Pradesh, India. *Wat Air Soil Pollut* 202:45–56.
473 <https://doi.org/10.1007/s11270-008-9957-8>

474 Koske RE, Tessier B (1983) A convenient, permanent slide mounting medium. *Mycol Soc Am Newsl* 34:59

475 Krishnamoorthy R, Kim CG, Subramanian P, Kim KY, Selvakumar G, Sa TM (2015) Arbuscular mycorrhizal
476 fungi community structure, abundance and species richness changes in soil by different levels of heavy metal
477 and metalloid concentration. *PloS one*, 10:e0128784. <https://doi.org/10.1371/journal.pone.0128784>

478 Krüger M, Stockinger H, Krüger C, Schüßler A (2009) DNA-based species level detection of Glomeromycota:
479 one PCR primer set for all arbuscular mycorrhizal fungi. *New Phytol* 183:212–223.
480 <https://doi.org/10.1111/j.1469-8137.2009.02835.x>

481 Krüger M, Krüger C, Walker C, Stockinger H, Schüßler A (2012) Phylogenetic reference data for systematics
482 and phylotaxonomy of arbuscular mycorrhizal fungi from phylum to species level. *New Phytol* 193:970–984.
483 <https://doi.org/10.1111/j.1469-8137.2011.03962.x>

484 Long LK, Yao Q, Guo J, Yang RH, Huang YH, Zhu HH (2010) Molecular community analysis of arbuscular
485 mycorrhizal fungi associated with five selected plant species from heavy metal polluted soils. *Eur J Soil Biol*
486 46:288–294. <https://doi.org/10.1016/j.ejsobi.2010.06.003>

487 Mucina L (1997) Conspectus of classes of European vegetation. *Folia Geobot Phytotaxon* 32:117–172.
488 <https://doi.org/10.1007/BF02803738>

489 Myers N, Mittermeier RA, Mittermeier CG, da Fonseca GAB, Kent J (2000) Biodiversity hotspots for
490 conservation priorities. *Nature* 403:853–858.

491 Oehl F, Sieverding E, Palenzuela J, Ineichen K, Alves da Silva G (2011a) Advances in glomeromycota
492 taxonomy and classification. *IMA Fungus* 2:191–199. <https://doi.org/10.5598/imafungus.2011.02.02.10>

493 Oehl F, Silva GA, Goto BT, Sieverding E (2011b) Glomeromycota: three new genera, and glomoid species
494 reorganized. *Mycotaxon* 116:75–120. <https://doi.org/10.5248/116.75>

495 Öpik M, Vanatoa A, Vanatoa E, Moora M, Davison J, Kalwij JM, Reier Ü, Zobel M. (2010). The online
496 database MaarjAM reveals global and ecosystemic distribution patterns in arbuscular mycorrhizal fungi
497 (Glomeromycota). *New Phytol* 188: 223–241. <https://doi.org/10.1111/j.1469-8137.2010.03334.x>

498 Öpik M, Davison J, Moora M, Zobel M (2014) DNA-based detection and identification of Glomeromycota: the
499 virtual taxonomy of environmental sequences. *Botany* 92:135–147. <https://doi.org/10.1139/cjb-2013-0110>

500 Palenzuela J, Azcón-Aguilar C, Barea JM, Silva GA, Oehl F (2013) *Acaulospora pustulata* and *Acaulospora*
501 *tortuosa*, two new species in the Glomeromycota associated with endangered plants in Sierra Nevada
502 (southern Spain). *Nova Hedwigia* 97:305–319. <https://doi.org/10.1127/0029-5035/2013/0129>

503 Park H, Lee EH, Ka KH, Eom AH (2016) Community structures of arbuscular mycorrhizal fungi in soils and
504 plant roots inhabiting abandoned mines of Korea. *Mycobiology* 44:277–282.
505 <https://doi.org/10.5941/MYCO.2016.44.4.277>

506 Pawlowska TE, Błaszczowski J, Rühling, Å. (1996). The mycorrhizal status of plants colonizing a calamine spoil
507 mound in southern Poland. *Mycorrhiza* 6:499–505. <https://doi.org/10.1007/s005720050154>

508 Ronquist F, Teslenko M, Van Der Mark P et al (2012) MrBayes 3.2: efficient Bayesian phylogenetic inference
509 and model choice across a large model space. *Syst Biol* 61:539–542. <https://doi.org/10.1093/sysbio/sys029>

510 Regvar M, Likar M, Piltaver A, Kugonič N, Smith JE (2010) Fungal community structure under goat willows
511 (*Salix caprea* L.) growing at metal polluted site: The potential of screening in a model phytostabilisation
512 study. *Plant Soil* 330:345–356. <https://doi.org/10.1007/s11104-009-0207-7>

513 Sánchez-Castro I, Gianinazzi-Pearson V, Cleyet-Marel JC, Baudoin E, van Tuinen D (2017) Glomeromycota
514 communities survive extreme levels of metal toxicity in an orphan mining site. *Sci Tot Environ* 598:121–128.
515 <https://doi.org/10.1016/j.scitotenv.2017.04.084>

516 Schenck NC, Pérez Y (1990) Manual for the identification of VA mycorrhizal fungi, 3rd edn. Synergistic,
517 Gainesville, Fla.

518 Sieverding E (1991) Vesicular-arbuscular mycorrhizal management in tropical agrosystems. Deutsche
519 Gesellschaft für Technische Zusammenarbeit 224. Hartmut Bremer Verlag, Friedland, Germany

520 Sieverding E, Silva GA, Berndt R, Oehl F (2014) *Rhizoglomus*, a new genus in the Glomeraceae. *Mycotaxon*
521 129:373–386. <https://doi.org/10.5248/129.373>

522 Silva GA, Lumini E, Maia LC, Bonfante P, Bianciotto V (2006) Phylogenetic analysis of *Glomeromycota* by
523 partial LSU rDNA sequences. *Mycorrhiza* 16:183–189. <http://dx.doi.org/10.1007/s00572-005-0030-9>

524 Sousa NM, Veresoglou SD, Oehl F, Rillig MC, Maia, LC (2018). Predictors of arbuscular mycorrhizal fungal
525 communities in the Brazilian tropical dry forest. *Microb Ecol* 75: 447–458. [https://doi.org/10.1007/s00248-](https://doi.org/10.1007/s00248-017-1042-7)
526 017-1042-7

527 Spain JL (1990) Arguments for diagnoses based on unaltered wall structures. *Mycotaxon* 38:71–76.

528 Stockinger H, Krüger M, Schübler A (2010) DNA barcoding of arbuscular mycorrhizal fungi. *New Phytol* 187:
529 461–474. <https://doi.org/10.1111/j.1469-8137.2010.03262.x>

530 Sudová R, Sýkorová Z, Rydlová J, Čtvrtlíková M, Oehl F (2015) *Rhizoglossum melanum*, a new arbuscular
531 mycorrhizal fungal species associated with submerged plants in freshwater lake Avsjøen in Norway. *Mycol*
532 *Progress* 14:9. <https://doi.org/10.1007/s11557-015-1031-5>

533 Sun Y, Zhang X, Wu Z, Hu Y, Wu S, Chen B (2016) The molecular diversity of arbuscular mycorrhizal fungi in
534 the arsenic mining impacted sites in Hunan Province of China. *J Environ Sci* 39:110–118.
535 <https://doi.org/10.1016/j.jes.2015.10.005>

536 Symanczik S, Błaszowski J, Chwat G, Boller T, Wiemken A, Al-Yahya’ei M (2014) Three new species of
537 arbuscular mycorrhizal fungi discovered at one location in a desert of Oman: *Diversispora omaniana*,
538 *Septoglossum nakheelum* and *Rhizophagus arabicus*. *Mycologia* 106:243–259.
539 <https://doi.org/10.3852/106.2.243>

540 Symanczik S, Al-Yahya’ei MN, Kozłowska A, Ryszka P, Błaszowski J (2018) A new genus, *Desertispora*, and
541 a new species, *Diversispora sabulosa*, in the family Diversisporaceae (order Diversisporales, subphylum
542 Glomeromycotina). *Mycol Progress* 17:437–449. <https://doi.org/10.1007/s11557-017-1369-y>

543 Tamura K, Stecher G, Peterson D, Filipski A, Kumar S (2013) MEGA6: Molecular Evolutionary Genetics
544 Analysis Version 6.0. *Mol Biol Evol* 30:2725–2729. <https://doi.org/10.1093/molbev/mst197>

545 Tedersoo L, Sánchez-Ramírez S, Urmas Kõljalg U, Bahram M, Döring M, Schigel D, et al. (2018). High-level
546 classification of the Fungi and a tool for evolutionary ecological analyses. *Fung Div* 90:135–159.
547 <https://doi.org/10.1007/s13225-018-0401-0>

548 Thaxter R (1922) A revision of the Endogoneae. *Proc Amer Acad Arts* 57:291–351.
549 <https://doi.org/10.2307/20025921>

550 Turnau K, Ryszka P, Gianinazzi-Pearson V, van Tuinen D (2001). Identification of arbuscular mycorrhizal fungi
551 in soils and roots of plants colonizing zinc wastes in southern Poland. *Mycorrhiza* 10:169–174.
552 <https://doi.org/10.1007/s005720000073>

553 Turrini A, Giovannetti M (2012) Arbuscular mycorrhizal fungi in national parks, nature reserves and protected
554 areas worldwide: a strategic perspective for their in situ conservation. *Mycorrhiza* 22:81–97.
555 <https://doi.org/10.1007/s00572-011-0419-6>

556 Vallino M, Massa N, Lumini E, Bianciotto V, Berta G, Bonfante P (2006) Assessment of arbuscular mycorrhizal
557 fungal diversity in roots of *Solidago gigantea* growing in a polluted soil in Northern Italy. *Environ Microbiol*
558 8:971–983. <https://doi.org/10.1111/j.1462-2920.2006.00980.x>

559 Vogel-Mikuš K, Pongrac P, Kump P, Necemer M, Regvar M (2006) Colonisation of a Zn, Cd and Pb
560 hyperaccumulator *Thlaspi praecox* Wulfen with indigenous arbuscular mycorrhizal fungal mixture induces
561 changes in heavy metal and nutrient uptake. *Environ Pollut* 139:362–371.
562 <https://doi.org/10.1016/j.envpol.2005.05.005>

563 Wei Y, Chen Z, Wu F, Li J, ShangGuan Y, Li F, Zeng QR, Hou, H (2015) Diversity of arbuscular mycorrhizal
564 fungi associated with a sb accumulator plant, ramie (*Boehmeria nivea*), in an active Sb mining. *J Microbiol*
565 *Biotechnol* 25:1205–1215. <https://doi.org/10.4014/jmb.1411.11033>

566 Whitfield L, Richards AJ, Rimmer DL (2004) Relationships between soil heavy metal concentration and
567 mycorrhizal colonisation in *Thymus polytrichus* in northern England. *Mycorrhiza* 14:55–62.
568 <https://doi.org/10.1007/s00572-003-0268-z>

569 Wu FY, Bi YL, Leung HM, Ye ZH, Lin XG, Wong MH (2010) Accumulation of As, Pb, Zn, Cd and Cu and
570 arbuscular mycorrhizal status in populations of *Cynodon dactylon* grown on metal-contaminated soils. *Appl*
571 *Soil Ecol* 44:213–218. <https://doi.org/10.1016/j.apsoil.2009.12.008>

572 Yang Y, Song Y, Scheller HV, Ghosh A, Ban Y, Chen H, Tang M (2015) Community structure of arbuscular
573 mycorrhizal fungi associated with *Robinia pseudoacacia* in uncontaminated and heavy metal contaminated
574 soils. *Soil Biol Biochem* 86:146–158. <https://doi.org/10.1016/j.soilbio.2015.03.018>

575 Zarei M, Saleh-Rastin N, Jouzani GS, Savaghebi G, Buscot F (2008) Arbuscular mycorrhizal abundance in
576 contaminated soils around a zinc and lead deposit. *E J Soil Biol* 44:381–391.
577 <https://doi.org/10.1016/j.ejsobi.2008.06.004>

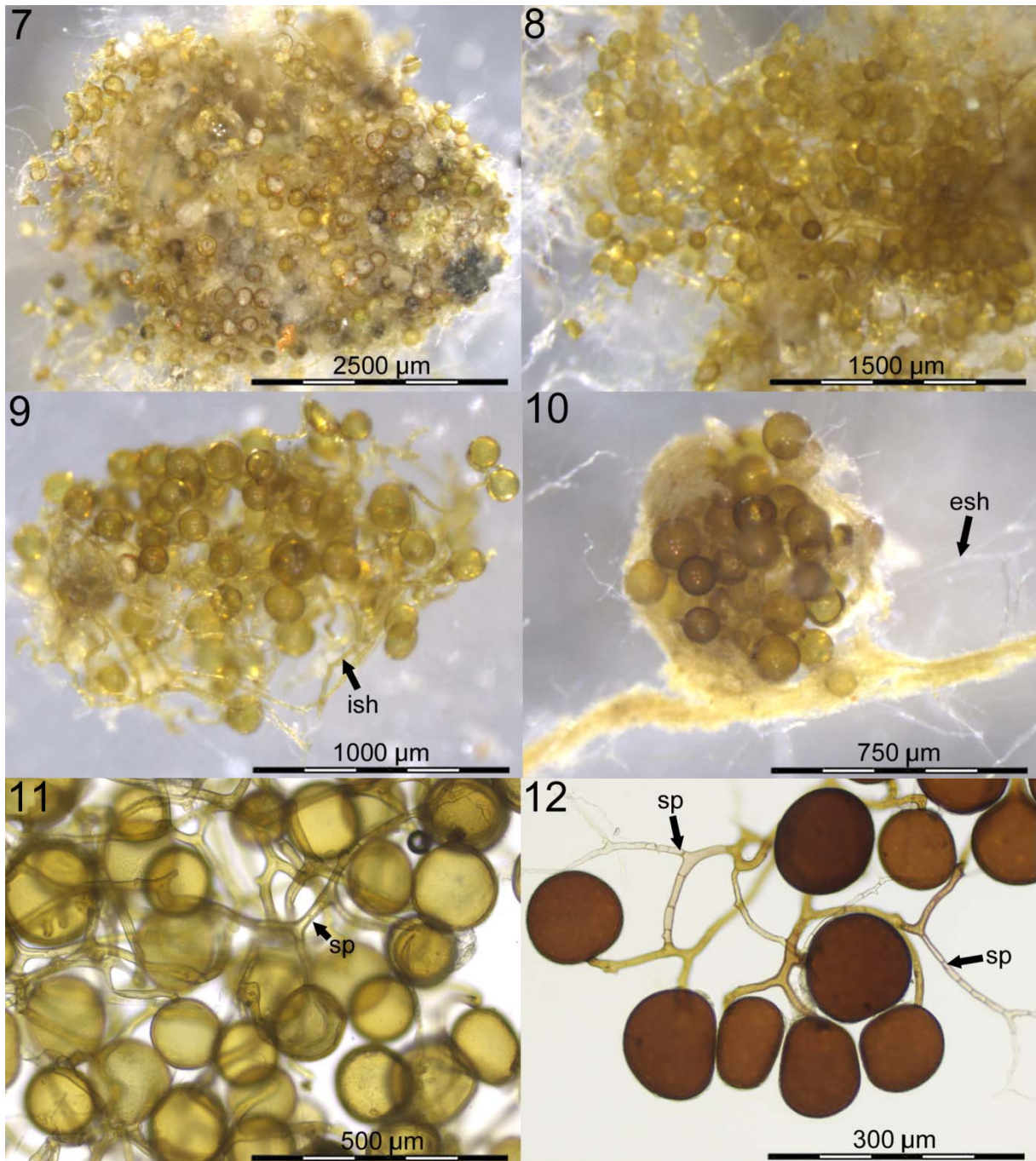
578

579 **Figure legends**



580
581 **Figs 1-6**

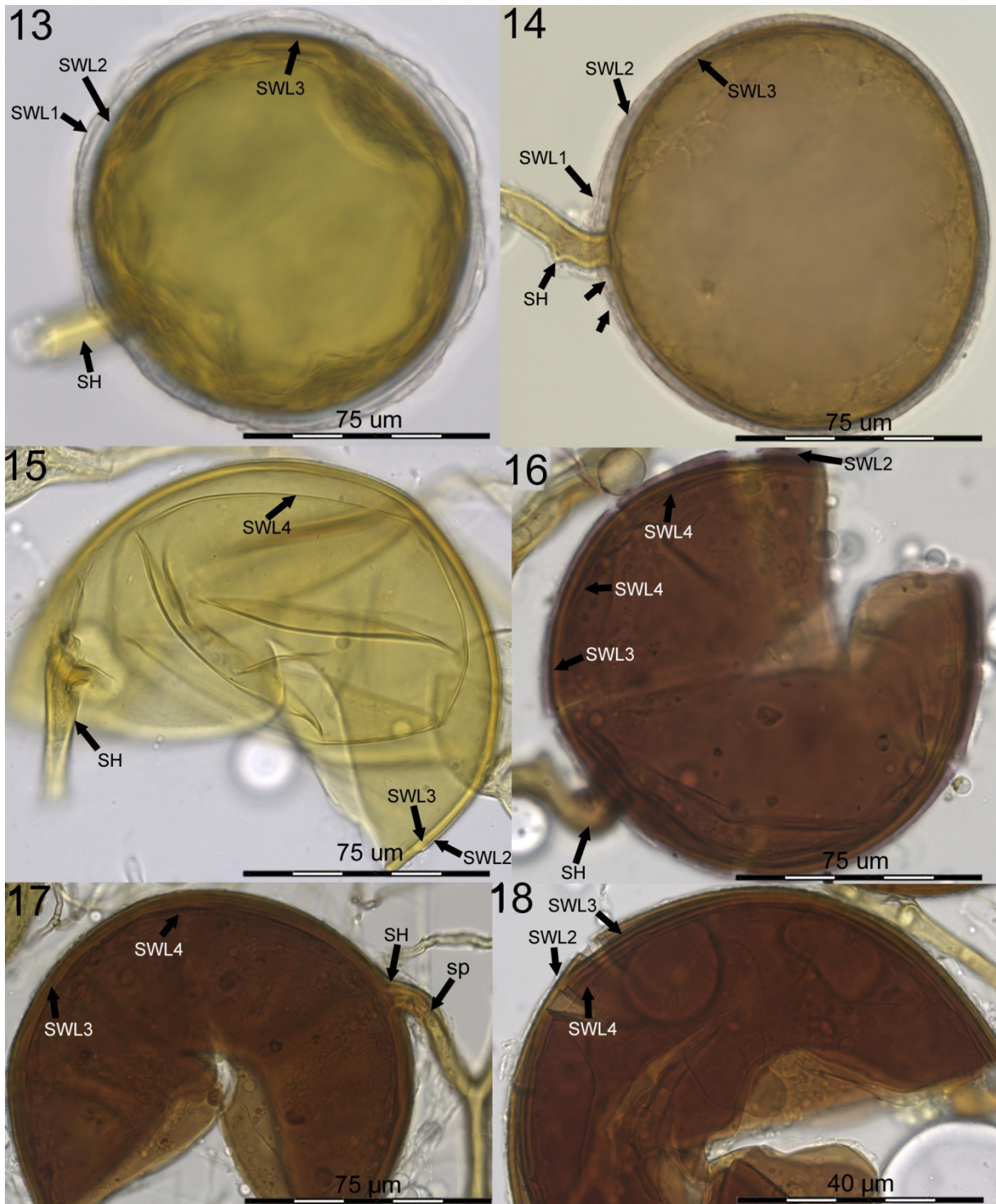
582 Isolation of *Rhizoglyphus venetianum* from Sacca San Biagio island, Venice, Italy. 1. Sacca San Biagio island (on
583 the left) with the perimetral embankments and the vegetation coverage and Venice's living quarters in the
584 background. 2. Ashes collected from the island. 3. *Senecio inaequidens* trap cultures using plants collected in the
585 island. 4-5. Production of extraradical mycelium from *Trifolium alexandrinum* roots used as bite plants in the
586 sandwich system (root diameter ca. 500 μm). 6. Spores of *R. venetianum* produced in the type culture (single
587 spore diameter ca. 80–140 μm).



588

589 **Figs 7-12**

590 *Rhizoglyphus venetianum*. 7–10. Sporocarps in water isolated from the rhizosphere of *Trifolium alexandrinum*
 591 from the single species culture of the type. Intrasporocarpic hyphae (ish) are generally pigmented, while
 592 extrasporocarpic hyphae (esh) are hyaline to subhyaline. 11. Sporocarp fragment mounted in PVLG. 12.
 593 Sporocarp fragment mounted in PVLG + Melzer's reagent. Several septa (sp) can be observed on
 594 intrasporocarpic hyphae and especially at the transition between extra- and intrasporocarpic hyphae.

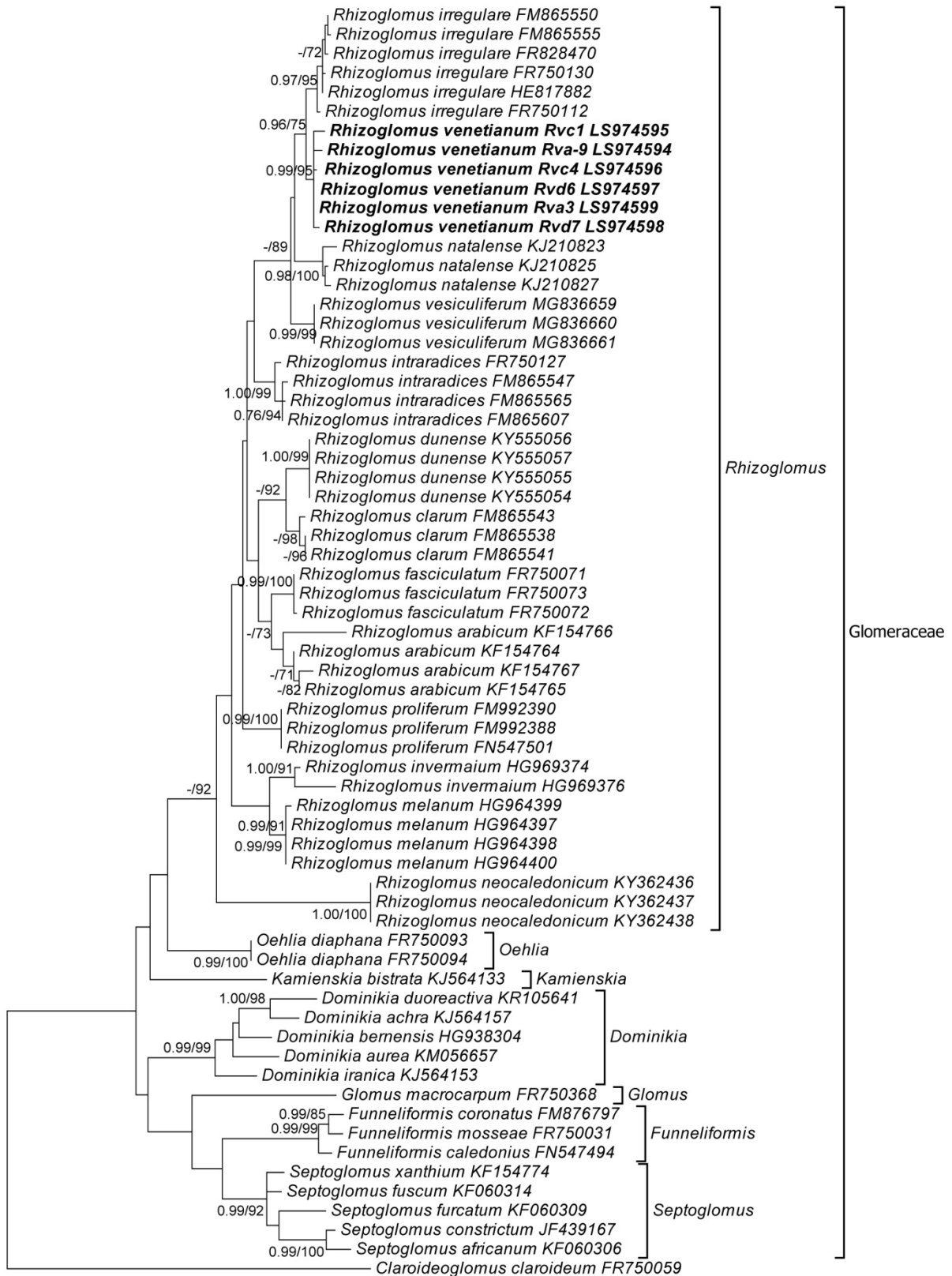


595

596 **Figs 13-18**

597 *Rhizoglosum venetianum*. 13–15. Uncrushed and crushed spores in PVLG. Spores with four layers (SWL1-4),
 598 cylindrical to slightly funnel-shaped subtending hyphae (SH) and open pores at the spore base. Sometimes a
 599 septum (sp) can be detected at some distance to the spore base. 16–18. Spores mounted in PVLG + Melzer's
 600 reagent. SWL1 and SWL2 stain pinkish to pinkish purple, while SWL3 stain purple.

601



602
603 **Fig. 19**

604 Maximum likelihood phylogenetic tree of glomeromycotan sequences obtained using the GTR+G model. The
605 analysis is based on partial SSU, ITS, and partial LSU region of the nuclear rDNA sequences (1763 characters;

606 SSUmCf3-LSUmBr1 fragment) and involved 66 nucleotide sequences. The Bayesian posterior probabilities and
607 ML bootstrap values are shown near the branches, respectively, when they exceed 0.50 and 70% (1000
608 replications). Sequences of the new species obtained in the present study are shown in bold, and their accession
609 numbers are prefixed with clone identifiers. Different genera and families are indicated in brackets. The tree is
610 rooted by a sequence of *Claroideoglomerus claroideum*.

611

612 **Author contributions**

613 The work was conceived by M.G. and A.T. A.T. isolated and carried out the trap cultures. M.S. and A.T. carried
614 out the molecular and phylogenetic analysis. F.O. performed the morphological description. A.T., F.O and M.G.
615 carried out the manuscript preparation for submission. All authors commented on the final draft of the
616 manuscript.

617